

Enhanced DNA Accessibility and Increased DNA Damage Induced by the Absence of Poly(ADP-ribose) Hydrolysis[†]

Yiran Zhou, Xiaoxing Feng, and David W. Koh*

Department of Pharmaceutical Sciences, College of Pharmacy, Washington State University, Pullman, Washington 99164

Received June 17, 2010; Revised Manuscript Received July 21, 2010

ABSTRACT: Poly(ADP-ribose) (PAR) is a therapeutic target primarily identified through inhibiting its synthesis by PAR polymerase-1 (PARP-1). However, inhibiting its hydrolysis by PAR glycohydrolase (PARG) has therapeutic potential in cancer. Unknown is the effect of elevated PAR levels on cellular processes and if this effect can enhance the therapeutic value of PARG. Here, we demonstrate in PARG null embryonic trophoblast stem (TS) cells that the absence of PAR hydrolysis led to PAR-modified histones H1, H2A, and H2B. To determine if this led to the differential vulnerability of DNA to modification, TS cells were treated with DNA-modifying agents. The results demonstrate increased DNA laddering by micrococcal nuclease and an increased amount of DNA intercalation by acridine orange in PARG null-TS cells. This increased access to PARG null-TS cell DNA was further verified by the detection of increased DNA damage following treatment with UV radiation and a minimal dose of the DNA-alkylating agent *N*-methyl-*N'*-nitro-*N*-nitrosoguanidine. Further, this DNA damage was predominantly unrepaired 12 h after treatment in PARG null-TS cells. Finally, TS cells were treated with DNA-modifying chemotherapeutic agents. The results demonstrate up to 4-fold increases in cell death in PARG null-TS cells after treatment with epirubicin or sub-IC₅₀ doses of cisplatin and cyclophosphamide. Taken together, we provide compelling evidence that increased DNA access induced by the absence of PARG enhances the efficacy of DNA-modifying agents. Thus, this study demonstrates that greater DNA accessibility, increased DNA damage, and increased cell death all contribute to the PARG null cell phenotype in response to genotoxic stress.

In response to DNA damage, polymers of ADP-ribose [poly(ADP-ribose) or PAR]¹ are synthesized by PAR polymerases (PARPs) to covalently modify nuclear protein acceptors (1). These acceptors include chromatin structural proteins, such as PARP-1 (2), histone H1 (3), and histone H2A/H2B (4). PAR is primarily removed from these proteins by the high specific activity of PAR glycohydrolase (PARG) (5–7), although an ADP-ribose hydrolase-like (ARH3) protein has also been shown to catalyze the hydrolysis of PAR to a lesser extent (8). Therefore, PARG catalytic activity is essential to the cell due to the high levels of PAR that are stimulated following DNA damage (9). PARG activity thus completes the majority of intracellular poly(ADP-ribosyl)ation cycles. Completed PAR cycles lead to the proper cellular response to genotoxic stress, including the facilitation of DNA repair (10, 11) or the induction of cell death (12). Thus, PAR has an important role in maintaining the fidelity of the genome (13).

Due to this role, PAR has been identified as a therapeutic target in several conditions, including cancer (14). However, most studies have focused on evaluating the chemotherapeutic potential of inhibiting PAR synthesis by targeting the PARPs. PARP

inhibitors effectively decrease PAR levels and are promising chemosensitizing agents due to their ability to inhibit DNA base-excision repair (10). They also hold promise in treating breast cancer tumors containing mutations in the breast cancer 2, early onset (BRCA2) gene (15). Conversely, inhibiting PARG is emerging as another chemotherapeutic strategy. Genetic PARG hypomorphs (16), partial genetic knockdown of PARG that leads to uncoordinated PARP/PARG activities (17), or RNAi knockdown (18) of PARG leads to increased cell death following DNA damage. We previously demonstrated that the absence of PARG led to embryonic trophoblast stem (TS) cell hypersensitivity to low-dose DNA-damaging agents (19). Thus, PARG appears to be a favorable target to induce cell death.

The metabolism of PAR mediates several cellular processes, including chromatin dynamics (2, 20), DNA replication and repair (21), and telomere maintenance (22). It is not known if the alteration of these or other PAR-mediated cellular processes leads to the observed PARG null cell hypersensitivity to low dose DNA-damaging agents. One possibility is the aforementioned alteration of chromatin structure. The PARPs induce chromatin decondensation via the PAR modification of chromatin structural proteins (2, 20). In vitro, heterologous PARG treatment reverses the PAR-induced chromatin decondensation by catalyzing the hydrolysis of PAR from histones and PARP-1 (2, 20). Thus, the possibility exists that a deficiency in PARG leads to chromatin structural changes due to the irreversible PAR modification of DNA-binding proteins. Further, this change in chromatin structure may lead to the enhanced sensitivity of DNA to DNA-modifying agents. The therapeutic significance of this scenario is particularly valuable in cancer, since inhibiting

[†]This work was supported by the American Cancer Society (IRG-77-003-26) and the Pharmaceutical Research and Manufacturers of America (PhRMA) Foundation.

*Address correspondence to this author. Phone: 509-335-7663. Fax: 509-335-5902. E-mail: dwkoh@wsu.edu.

Abbreviations: PAR, poly(ADP-ribose) or ADP-ribose polymer; PARG, poly(ADP-ribose) glycohydrolase; PARP, poly(ADP-ribose) polymerase; TS cell, embryonic trophoblast stem cell; BZ, benzamide; MNNG, *N*-methyl-*N'*-nitro-*N*-nitrosoguanidine; CPD, cyclobutane pyrimidine dimer; CIS, cisplatin; CPA, cyclophosphamide; EPI, epirubicin.

PARG may provide a potential method to increase the access of DNA-modifying anticancer agents to DNA. These cellular effects have the potential to provide a new basis that elevates PARG as a more favorable target in the chemotherapeutic treatment of cancer.

Our data here demonstrate that the absence of PARG led to the presence of PAR-modified chromatin structural proteins. Also, for the first time, we demonstrate increased access of DNA-modifying agents to DNA in the absence of PARG. Further, this resulted in an enhanced level of DNA damage following different modalities of DNA-damaging treatments. Finally, we show that PARG disruption significantly potentiated the cell death induced by currently utilized DNA-modifying chemotherapeutic agents.

EXPERIMENTAL PROCEDURES

Materials. *N*-Methyl-*N'*-nitro-*N*-nitrosoguanidine (MNNG) was purchased from AccuStandard (New Haven, CT). Protease inhibitors, acridine orange, cisplatin, epirubicin, and cyclophosphamide were all purchased from Calbiochem (La Jolla, CA). Micrococcal DNA nuclease was from New England Biolabs (Ipswich, MA). Primary antibodies utilized were monoclonal anti-PAR (clone 10H) (Tulip Biolabs, West Point, PA), polyclonal anti-PAR (96-10) (Trevigen, Gaithersburg, MD), polyclonal anti-histone H2A and H2B (Santa Cruz Biotech, Santa Cruz, CA), monoclonal anti-histone H1 (Millipore, Billerica, MA), and monoclonal anti-cyclobutane pyrimidine dimer (CPD) (Cosmo Bio USA, West Carlsbad, CA). Secondary antibodies utilized were horseradish peroxidase- (HRP-) conjugated goat anti-rabbit and anti-mouse (Sigma, St. Louis, MO) and Oregon Green-conjugated anti-mouse (Invitrogen, Carlsbad, CA). Protease inhibitor cocktail tablets (Complete EDTA-free) were from Roche (Mannheim, Germany).

Embryonic Trophoblast Stem (TS) Cell Culture. Wild-type and PARG null-TS cells were derived and cultured as previously reported (19). Benzamide (BZ), a PAR synthesis inhibitor, was required to maintain the viability of the PARG null-TS cell line.

Immunoprecipitation of PAR and Histones. TS cells were cultured \pm BZ for 3 days and harvested with trypsin. Cells were then lysed by brief sonication in ice-cold lysis buffer (25 mM Tris-HCl, pH 7.5, 150 mM NaCl, 1% NP-40, 1 mM EDTA, 1 mM EGTA, and protease inhibitor cocktail), and the extracts were placed on ice for 30 min. After centrifugation (13000 rpm for 15 min), the supernatants were cleared by applying a 50% (v/v) slurry of protein A-Sepharose resin (Invitrogen) for 2 h at 4 °C. The extracts were then incubated with the indicated antibodies at 4 °C for 2 h. The immunoprecipitation complexes were isolated with protein A-Sepharose resin at 4 °C overnight and washed three times with lysis buffer. The bound proteins were eluted and denatured with SDS loading buffer at 100 °C for 5 min. The proteins were then resolved on SDS-PAGE and subjected to immunoblot analysis.

Immunoblot Analyses. Samples (20 μ g) were subjected to 7% or 12% SDS-PAGE and transferred to nitrocellulose by semidry transfer (25 V for 1 h) using a Trans-blot SD apparatus (Bio-Rad, Hercules, CA). Membranes were blocked with PBS + 0.1% Tween-20 containing 5% milk for 1 h and incubated with primary antibody (1:1000) overnight at 4 °C. Membranes were then washed with PBS-Tween three times and incubated with HRP-conjugated goat anti-rabbit or anti-mouse antibody (1:10000) for 1 h. The blot was washed as before, and chemiluminescence was initiated using the Supersignal West Pico

reagents (Pierce, Rockford, IL). Immunoblots were then developed by film or on a Chemidoc gel imager (Bio-Rad).

Micrococcal DNA Nuclease (MNase) Digestion. The MNase digestion of TS cells was performed as previously described (23), except that the TS cells were homogenized in hypotonic buffer (10 mM Tris-HCl, pH 8.0, 10 mM MgCl₂, 1 mM DTT, 25% glycerol, 0.2% NP-40, 0.5 μ M spermidine, and protease inhibitor cocktail), and the resulting nuclei were treated with 5 units of MNase for 5 min. DNA was purified with phenol/chloroform and subjected to electrophoresis (1 μ g/lane) on a 1.2% agarose gel.

DNA Intercalation with Acridine Orange. TS cells were grown \pm BZ for 3 days, harvested with trypsin, washed with PBS, and stained with 10 μ g/mL acridine orange for 10 min. Total fluorescence intensity (FL1 channel) was measured using a FACSCalibur flow cytometer (BD, Franklin Lakes, NJ). Mean fluorescence values were calculated using FlowJo software (Tree Star, Ashland, OR).

Detection of DNA Damage following UV Radiation. TS cells were seeded onto sterile glass coverslips and placed in 24-well plates. The cells were then cultured \pm BZ for 2 days. For UV treatment, cells were washed with PBS and irradiated using a low-pressure Hg lamp (model G30T8; Sylvania, Danvers, MA) at 10 J/m². The cells were fixed with 4% formalin in PBS for 10 min, washed twice with PBS, permeabilized with 0.5% Triton X-100 in PBS for 5 min on ice, and washed twice with PBS. The cells were treated with 2 M HCl for 30 min to denature genomic DNA, washed five times with PBS, and blocked with 10% BSA/PBS for 30 min at 37 °C. Cells were then incubated for 2 h at 37 °C with monoclonal anti-CPD antibody (1:1500) in 3% BSA/PBS. After three PBS washes, cells were incubated with Oregon Green-conjugated anti-mouse antibody (1:1000) in 3% BSA/PBS for 45 min at 37 °C in the dark. Coverslips were washed three times with PBS, mounted on glass microscope slides containing DAPI, and visualized by confocal microscopy.

Detection of DNA Damage following DNA Alkylation. TS cells were cultured \pm BZ for 3 days and treated with MNNG for 5 min. After 30 min, DNA damage was assessed using the single-cell gel electrophoresis (Comet) assay using the CometAssay electrophoresis system (Trevigen). Briefly, 0.5% low melting point agarose was mixed with approximately 500 cells and spread onto two-well CometSlides. Once solidified, the slides were placed in lysis solution (10 mM Tris base, 2.5 M NaCl, 0.1 M EDTA, pH 10, 1% sodium lauryl sarcosinate, and 1% Triton X-100) at 4 °C for 30 min and equilibrated in alkaline solution (200 mM NaOH and 1 mM EDTA) for 30 min to unwind the DNA. The slides were then transferred to the electrophoresis unit and subjected to 21 V for 30 min. Nuclei were stained with SYBR Green, and the images were analyzed using CometScore software (TriTek Corp., Sumerduck, VA). For DNA damage quantifications, “% DNA in tail” is defined as 100 – percent DNA in comet head; “tail moment” is defined as comet tail length \times fraction of total DNA in the tail. Both parameters are linearly correlated to DNA strand break frequency (24, 25).

Cell Death Assays. TS cells were grown \pm BZ for 2 days in 24-well plates and treated with cyclophosphamide, cisplatin, or epirubicin at the indicated doses and exposures (Table 1). After the treatment exposure period, cells were washed once with media and once with PBS and incubated in growth media at 37 °C. Twenty to twenty-four hours after treatment, cells were harvested with trypsin, washed with PBS, and resuspended in PBS. Cell suspensions were then stained with annexin V-FITC/propidium

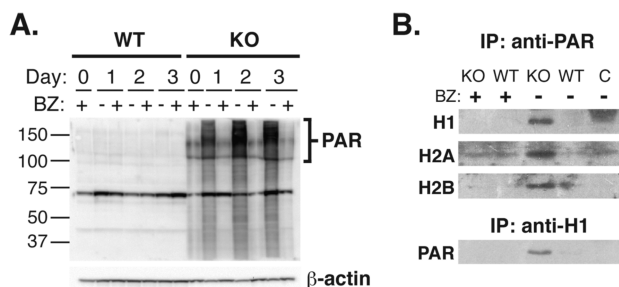


FIGURE 1: Detection of PAR-modified histones in PARG null murine TS cells. (A) Immunoblotting detection of PAR in TS cells. TS cells were cultured in growth medium lacking benzamide (BZ) for 1–3 days. TS cell lysates were then probed with anti-PAR polyclonal antibody. If present, the majority of PAR lies within the bracketed region (~90–200 kDa). Note: The protein band near M_r 66000 is the immunodetection of BSA, which was utilized in the production of the anti-PAR antibody. (B) TS cell extracts were withdrawn from BZ for 3 days and immunoprecipitated using monoclonal anti-PAR (clone 10H) antibody or mouse IgG (negative control), followed by Western analysis with anti-histone H1, H2A, and H2B. The TS cell extracts were also immunoprecipitated using anti-histone H1 antibody followed by Western analysis with anti-PAR. Key: WT, wild-type TS cells; KO, PARG null-TS cells; C, mouse IgG negative control.

iodide (Vybrant apoptosis assay kit no. 3; Invitrogen) according to the manufacturer's protocol and analyzed by FACS as performed previously (19). Total cell death was quantified by adding the percentage of cells detected in the upper left, upper right, and lower right quadrants in the FACS dot plots.

RESULTS

Detection of PAR-Modified Histones in the Absence of PARG. We previously reported that the PARG null phenotype is embryonic lethality (19). However, PARG null-TS cells, the only genetic model system available to date where PARG is completely absent, were successfully derived from PARG null blastocysts. However, the PAR synthesis inhibitor benzamide (BZ) is required in the growth medium of PARG null-TS cells in order to maintain viability. Previously, we demonstrated that PAR accumulates in a time-dependent fashion in unstressed cells after BZ withdrawal (19). Accordingly, increased levels of PAR were observed in PARG null-TS cells from days 1–3 after BZ withdrawal (Figure 1A).² No accumulation of PAR was observed in wild-type TS cells \pm BZ or PARG null-TS cells +BZ.

Three well-known acceptors of the PAR modification are the linker histone H1 (3) and the core nucleosomal histones H2A and H2B (4). Therefore, we analyzed the PAR-modified proteins in PARG null-TS cells –BZ to determine if PAR-modified histones were present. Extracts were subjected to immunoprecipitation (IP) using monoclonal anti-PAR antibody and probed for the presence of histones H1, H2A, and H2B (Figure 1B). In PARG null-TS cells –BZ, each histone was successfully detected by immunoblot (Figure 1B), which indicates that these histones were PAR-modified. PAR-modified histones were not observed in wild-type or PARG null-TS cells +BZ, which verifies the inhibition of PAR synthesis by BZ. Further, PAR-modified histones were not detected in wild-type cells –BZ after IP with anti-PAR antibody. This demonstrates that in wild-type cells capable of catalyzing the synthesis of PAR (i.e., in the absence of BZ), the

presence of functional PARG prevents the accumulation of PAR-modified histones. Taken together, the results demonstrate the presence of PAR-modified histones H1, H2A, and H2B in PARG null-TS cells due to the failure to catalyze the hydrolysis of PAR.

To further verify the presence of PAR-modified histones in PARG null-TS cells –BZ, the extracts were subjected to IP using anti-histone H1 antibody. The immunoprecipitated proteins were then probed for the presence of PAR (Figure 1B). In PARG null-TS cells –BZ, PAR-modified histone H1 was successfully detected using anti-PAR antibody. No PAR-modified histone H1 was observed in wild-type cells \pm BZ or PARG null-TS cells +BZ. Thus, the results demonstrate the presence of PAR-modified histone H1 in PARG null-TS cells –BZ following the IP of histone H1. Further, the results confirm the previous observation of PAR-modified histone H1 after the IP of PAR.

Increased DNA Accessibility Induced by the Absence of PARG. Histones H1, H2A, and H2B are positively charged proteins important for binding and assembling negatively charged DNA into highly compacted nucleosomal units. The PAR modification of DNA-binding proteins disrupts their interaction with DNA due to the charge repulsion of DNA and the highly anionic PAR (which contains two negatively charged phosphate groups per ADP-ribose unit) (26). This leads to the dissociation of the histone octamer from DNA. To determine if the elevated levels of PAR-modified histones due to the absence of PARG resulted in a change in DNA accessibility, we analyzed the susceptibility of TS cell DNA to micrococcal DNA nuclease (MNase). TS cells were cultured –BZ for 1–3 days and treated with MNase. Analysis of the resulting DNA fragments from PARG null-TS nuclei cultured –BZ for 2–3 days indicated nucleosomal laddering. This demonstrates a greater susceptibility of DNA from PARG null-TS cells –BZ to MNase digestion (Figure 2A). No significant laddering was observed in wild-type TS cells \pm BZ or PARG null-TS cells +BZ. Because this change in DNA susceptibility occurred only in PARG null-TS cells, this effect was mediated by the absence of PARG. Thus, the results demonstrate that PARG inhibition leads to the greater DNA access of MNase.

Increased Susceptibility of PARG Null-TS Cell DNA to Intercalation. To further verify increased DNA access, TS cells were treated with the DNA-intercalating agent acridine orange. Acridine orange intercalates into double-stranded DNA and produces green fluorescence with a maximal emission at 526 nm (23). PARG null-TS cells –BZ displayed an increase in fluorescence as compared to wild-type \pm BZ and PARG null-TS +BZ (Figure 2B), suggesting that PARG null-TS cell DNA after BZ withdrawal was more accessible to the dye. After quantifying mean fluorescence values for each group, PARG null-TS cells –BZ (82.3) clearly exhibited the highest fluorescence as compared to the other experimental groups (WT +BZ, 61.4; WT –BZ, 57.7; KO +BZ, 64.7), which demonstrates the greatest amount of DNA intercalation. The results thus reveal that the absence of PARG leads to increased DNA intercalation by acridine orange.

Increased DNA Damage Due to the Absence of PARG. If PAR, by altering the interaction of DNA and DNA-binding proteins, leads to greater DNA access, it is expected to increase the efficacy of different modalities of DNA damage-inducing treatments. To investigate the ability of UV radiation to damage DNA in the absence of PARG, TS cells were grown \pm BZ for 2 days and treated with 10 J/m² UV radiation. UV exposure

²In Figure 1A, the protein band near M_r 66000 is the immunodetection of bovine serum albumin (BSA). The production of the anti-PAR (96-10) antibody was accomplished using BSA as the carrier protein and PAR as the hapten.

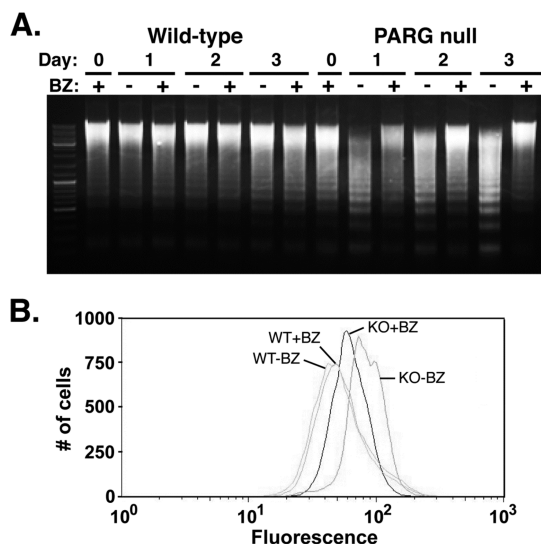


FIGURE 2: Increased nuclease digestion and intercalation of PARG null-TS cell DNA. (A) Micrococcal nuclease digestion of TS cell DNA after 1–3 days of BZ withdrawal. After each time point indicated, TS cell nuclei were isolated and treated with 5 units of micrococcal nuclease for 5 min. One microgram of DNA was loaded in each lane. (B) DNA intercalating agent treatment of TS cells after 3 days of BZ withdrawal. After 3 days –BZ, TS cells were treated with 10 μ g/mL acridine orange. The fluorescence intensity was measured by FACS. The mean fluorescence intensity calculated for each experimental group: WT +BZ, 61.4; WT –BZ, 57.7; KO +BZ, 64.7; KO –BZ, 86.0.

modifies thymine bases within DNA to form (6–4)-photoproducts and cyclobutane pyrimidine dimers (CPDs) (27). The results demonstrate that UV radiation produced minimal amounts of CPDs in wild-type TS cells (Figure 3A) as visualized by immunocytochemistry using a monoclonal anti-CPD antibody. However, in PARG null-TS cells –BZ, CPDs were more prevalent and widespread (green channel), indicating a greater amount of DNA damage as compared to wild type (Figure 3B). The results thus demonstrate increased amounts of UV-induced CPDs in the absence of PARG.

To investigate the ability of chemical mutagens to damage DNA in the absence of PARG, TS cells were treated with the DNA-alkylating agent MNNG. MNNG treatment leads to methylated DNA bases (28), as well as the alkylation of proteins (29). The resulting DNA damage was examined by the single cell gel electrophoresis (Comet) assay, a sensitive technique for analyzing and quantifying DNA damage in individual cells (30). Following electrophoresis, each cell resembles a comet with a distinct head and tail. Undamaged, intact DNA is contained in the head. Damaged DNA, which results in DNA strand breaks, migrates and produces the tail. As expected, no significant damage was observed in untreated TS cells due to the absence of tails (Figure 4A, left panels). Treatment with MNNG led to comet tails in wild-type and PARG null-TS cells –BZ, indicating DNA damage (Figure 4A, right panels). However, the tails in PARG null-TS cells were significantly larger (Figure 4A, white arrows), which illustrates a greater amount of migrated DNA. This demonstrates a greater amount of DNA damage induced in PARG null-TS cells as compared to wild-type cells after MNNG treatment. Further, the comet heads in wild-type TS cells after MNNG treatment were consistently larger than in PARG null-TS cells (Figure 4A, gray arrows), which indicates a greater amount of undamaged DNA in wild-type cells. To quantify the amount of DNA damage, “% DNA in tail” and “tail

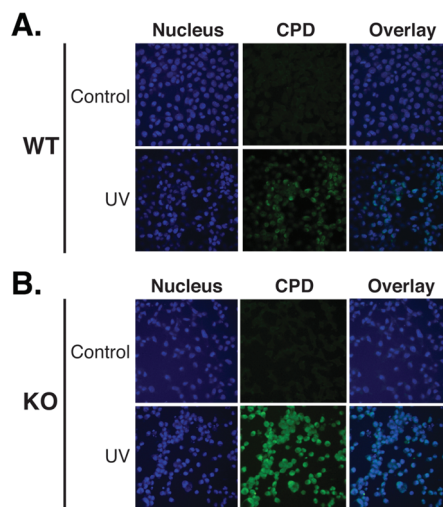


FIGURE 3: Detection of DNA damage in wild-type and PARG null-TS cells following UV radiation. TS cells were cultured –BZ for 2 days and treated with 10 J/m² UV radiation. The cells were labeled with DAPI nuclear DNA stain (blue channel) and monoclonal antibody against CPDs (green channel). (A) Wild-type TS cells. (B) PARG null-TS cells. The merge (bottom right) of the CPD and DAPI images indicates the successful detection of UV-induced DNA damage (cyan).

moment” values were determined. The calculated values indicate a 3.5-fold increase in “tail moment” and a 2.5-fold increase in “% DNA in tail” in PARG null-TS cells –BZ as compared to wild-type cells –BZ (Figure 4B). This provides quantitative evidence that a greater amount of DNA damage is produced in PARG null-TS cells –BZ. Taken together, the results provide qualitative and quantitative verification that the increased DNA access of DNA-modifying agents induced by the absence of PARG leads to greater amounts of DNA damage.

Increased DNA Damage Remains in PARG Null-TS Cells after a DNA Repair Period. The MNNG-treated TS cells were incubated at 37 °C for 12 h to allow DNA repair mechanisms to ensue. Following this DNA repair period, much of the DNA damage observed in wild-type TS cells was successfully repaired. This was demonstrated by a reduction in comet tails (Figure 4C, white arrow). The calculated “tail moment” and “% DNA in tail” values were also decreased in wild-type cells (Figure 4D). However, in PARG null-TS cells, the comet tails remained largely unchanged after the repair period (Figure 4C, bottom panel), indicating the continued presence of considerable amounts of DNA damage. Further, the “tail moment” and “% DNA in tail” values remained 2.7- and 2.0-fold higher than wild-type levels, respectively (Figure 4D). This demonstrates that most of the DNA damage induced by MNNG in the absence of PARG remained unrepaired after 12 h.

The Absence of PARG Leads to the Increased Efficacy of DNA-Modifying Chemotherapeutic Agents. Based on the previous studies, we investigated the ability of the absence of PARG to increase the ability of currently utilized DNA-modifying chemotherapeutic agents to induce cell death. TS cells were cultured \pm BZ and treated with the anticancer agents at the indicated doses and exposure times (Table 1), and cell death was quantified 20–24 h later by FACS. As shown in Figure 5, all of the chemotherapeutic drugs produced increased cell death in PARG null-TS cells –BZ. However, this increased cell death was abrogated when PARG null-TS cells were cultured +BZ, which suggests a role for PAR in the chemosensitization mechanism.

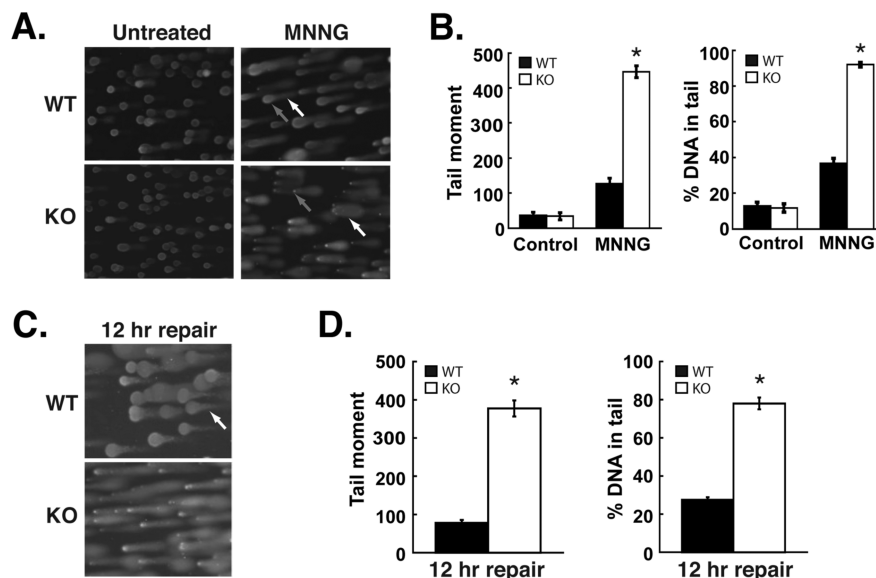


FIGURE 4: Detection of DNA damage in wild-type and PARG null-TS cells following DNA-alkylating agent treatment. (A) DNA damage was detected by the Comet assay, and representative images of untreated (left panels) and MNNG-treated TS cells (right panels) are shown. Comet heads indicate undamaged DNA (gray arrows), and comet tails demonstrate DNA damage (white arrows). (B) Quantification of DNA damage in TS cells after MNNG treatment. All images were utilized to quantify DNA damage using CometScore software. (C) MNNG-treated cells were analyzed by Comet assay after a 12 h repair period that followed the MNNG treatment. (D) DNA damage after the 12 h repair period was quantified as in (B). For all graphs, *, $P < 0.01$ WT vs KO (unpaired Student's t test); error bars are shown as SEM.

The amount of cell death produced by the anticancer agents in PARG null-TS cells +BZ was 2.0–4.0-fold greater than in wild-type cells +BZ (Table 1). It is worth noting that the doses utilized for cisplatin and cyclophosphamide were lower than the reported IC_{50} doses for each agent to inhibit the growth of cultured cells (31, 32). Further, the exposure time of epirubicin utilized (30 min) was considerably less than that previously reported (48 h) in cultured cells (33). Thus, the increased amount of cell death observed verifies that the absence of PARG leads to the increased efficacy of cisplatin, cyclophosphamide, and epirubicin to induce cell death.

DISCUSSION

This study reports, for the first time, specific intranuclear effects induced by the absence of PARG. These effects on DNA accessibility and DNA damage are shown to be mediated by PAR. Preventing the hydrolysis of PAR by the genetic disruption of the *Parg* gene leads to elevated levels of PAR-modified histones H1, H2A, and H2B. This leads to the increased DNA access of MNase and acridine orange to genomic DNA. Because MNase and acridine orange are two common techniques used to detect changes in chromatin structure (23, 34), it is probable that these effects also indicate a chromatin structural change. Further, it is well-known that PAR mediates chromatin structural dynamics. This is accomplished via the PAR modification of chromatin-binding proteins to induce chromatin decondensation (2, 20, 34) and the hydrolysis of PAR from these proteins to promote chromatin recondensation (2, 20). Thus, the possible chromatin structural change induced by the absence of PARG in this study most likely involves chromatin decondensation, since PARG activity is required for chromatin recondensation. It is therefore possible that this unpackaged, relaxed state of chromatin allows greater DNA accessibility. However, more studies will be required to verify these possibilities.

It is also probable that the PAR modification of other chromatin binding proteins is involved, such as histone H3 and

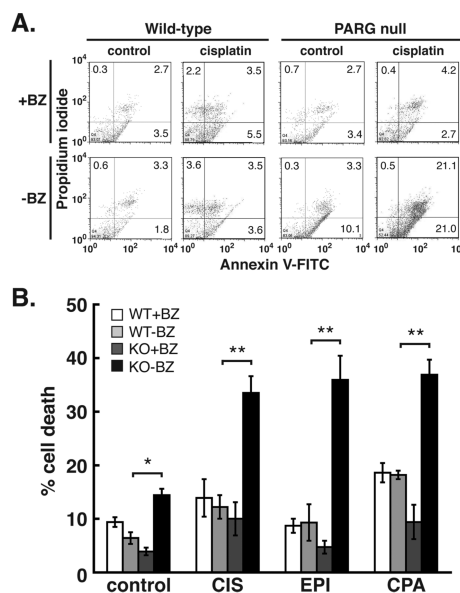


FIGURE 5: Treatment of PARG null-TS cells with DNA-modifying chemotherapeutic agents. (A) Representative FACS dot plots for wild-type and PARG null-TS cells cultured \pm BZ and treated with cisplatin (55 μ M for 2.5 h). (B) Quantification of cell death produced by cisplatin, epirubicin, and cyclophosphamide in TS cells by FACS. *, $P < 0.05$ WT +BZ vs KO +BZ (unpaired Student's t test); **, $P < 0.01$ WT +BZ vs KO +BZ; error bars are shown as SEM. Key: CIS, cisplatin; EPI, epirubicin; CPA, cyclophosphamide. The data represent four independent experiments.

PARP-1, both known to be acceptors of the PAR modification (3, 35). PARP-1 is a nuclear protein acceptor of the majority of PAR in the cell through an automodification reaction (35). Recently, it was shown to bind chromatin and promote its compaction, while automodified PARP-1 failed to bind and led to chromatin relaxation (2). Removal of PAR by exogenous PARG led to PARP-1 rebinding and chromatin recondensation. Other possibilities are noncovalent interactions that may

Table 1: Cell Death Induced by Chemotherapeutic Agents in the Absence of PARG

agent	DNA modification	dose (μM)	exposure time	fold increase in cell death ^a	IC ₅₀ (μM) ^b	ref
cyclophosphamide	alkylation	200	24 h	3.9	10000	30
cisplatin	cross-linking	55	2.5 h	2.7	230	31
epirubicin	intercalation	1.5	30 min	2.0	0.12 ^c	32

^aRepresents the amount of cell death in PARG null-TS cells cultured –BZ versus control cell death levels provided by wild-type TS cells cultured –BZ. ^bIC₅₀ is defined as the concentration of drug necessary to produce 50% inhibition of cell growth. ^cBased on exposure time of 48 h (see ref 32).

contribute to this effect on DNA, as PAR was shown to bind histones in vitro (36, 37). Most likely through ionic interactions, this association was disrupted by the hydrolysis of PAR by PARG (38). Thus, because the absence of PARG leads to the accumulation of intranuclear PAR-modified proteins, other contributing factors mediated by PAR are possible, including histone “shuttling” (38).

We provide the first evidence here that increased DNA damage can be induced by the inhibition of PARG. Both UV radiation and small-molecule chemical agents successfully led to increased DNA damage in the absence of PARG. In addition, the dose of MNNG utilized in these studies (5 μM) is most likely incapable of inducing widespread cytotoxicity alone. This dose is 10–60-fold lower than the normal MNNG dose utilized in cultured cells (7, 39). As demonstrated here, the combination of this low dose of MNNG and the absence of PARG produced a sizable amount of DNA damage that was not completely repaired. Although significant DNA damage was also observed in wild-type TS cells following 5 μM MNNG, a more significant percentage of this damage was successfully repaired (Figure 4C). Thus, the low levels of DNA damage and higher fraction of repaired DNA in wild-type TS cells after 12 h are in agreement with our previous data demonstrating <10% cell death in wild-type TS cells after low-dose MNNG treatment (19). Taken together, the studies demonstrate that the inhibition of PARG leads to the increased ability of DNA-damaging treatments to modify DNA.

We further demonstrate that these effects on DNA accessibility have the potential to be utilized for therapeutic gain. Low doses or exposures of the chemotherapeutic agents cisplatin, cyclophosphamide, and epirubicin all significantly increased cell death in PARG null-TS cells –BZ, which corroborates the results demonstrating increased DNA access and increased DNA damage in the absence of PARG. PARG is a potential chemotherapeutic target, as previous studies demonstrated increased cell death in cells deficient, but not completely lacking, in PARG (16, 17, 40). Our previous study contributed to these observations by demonstrating a profound amount of PARG null-TS cell death induced by sublethal doses of MNNG and menadione (19). However, the mechanism of this PARG null-TS cell hypersensitivity was unknown. Here, we provided insight into this phenotype by demonstrating a specific mechanism of PARG null-TS cell hypersensitivity that involves the PAR modification of chromatin-binding proteins that most likely involves the modulation of chromatin structure. It remains to be seen if this or other PAR-mediated cellular processes are the primary cause of the cytotoxic PARG null phenotype.

It is worth noting that we have demonstrated increased cell death in normal cells in the absence of PARG. The selective targeting of PARG inhibition in cancer cells, in addition to chemotherapy, would undoubtedly be the most beneficial strategy to improve the future treatment of cancer patients. Therefore, the selective targeting of PARG in cancer cells, in

order to minimize toxicity to normal cells, will be required in the future to elevate PARG into a bona fide chemotherapeutic target.

In summary, we demonstrate a PAR-induced increase in DNA accessibility that leads to increased DNA damage by UV or chemical DNA mutagens in the absence of PARG. These results provide preliminary validation that PARG is an attractive therapeutic target to induce cell death. However, PARG depletion studies in cancer cell models, specific targeting of cancer cells by PARG inhibition, and in vivo studies will be required to complete this validation.

ACKNOWLEDGMENT

We thank Dr. Christine Davitt and the Franceschi Microscopy and Imaging Center at Washington State University for technical assistance with the imaging studies. We also thank the laboratory of Dr. Michael J. Smerdon at Washington State University for assistance with the UV radiation studies. Special thanks are extended to Katie Eby and Alicia Proctor for general experimental assistance.

REFERENCES

1. Alvarez-Gonzalez, R., and Jacobson, M. K. (1987) Characterization of polymers of adenosine diphosphate ribose generated in vitro and in vivo. *Biochemistry* 26, 3218–3224.
2. Kim, M. Y., Mauro, S., Gevry, N., Lis, J. T., and Kraus, W. L. (2004) NAD⁺-dependent modulation of chromatin structure and transcription by nucleosome binding properties of PARP-1. *Cell* 119, 803–814.
3. Kreimeyer, A., Wielckens, K., Adamietz, P., and Hilz, H. (1984) DNA repair-associated ADP-ribosylation in vivo. Modification of histone H1 differs from that of the principal acceptor proteins. *J. Biol. Chem.* 259, 890–896.
4. Adamietz, P., and Rudolph, A. (1984) ADP-ribosylation of nuclear proteins in vivo. Identification of histone H2B as a major acceptor for mono- and poly(ADP-ribose) in dimethyl sulfate-treated hepatoma AH 7974 cells. *J. Biol. Chem.* 259, 6841–6846.
5. Brochu, G., Duchaine, C., Thibeault, L., Lagueux, J., Shah, G. M., and Poirier, G. G. (1994) Mode of action of poly(ADP-ribose) glycohydrolase. *Biochim. Biophys. Acta* 1219, 342–350.
6. Hatakeyama, K., Nemoto, Y., Ueda, K., and Hayaishi, O. (1986) Purification and characterization of poly(ADP-ribose) glycohydrolase. Different modes of action on large and small poly(ADP-ribose). *J. Biol. Chem.* 261, 14902–14911.
7. Jonsson, G. G., Jacobson, E. L., and Jacobson, M. K. (1988) Mechanism of alteration of poly(adenosine diphosphate-ribose) metabolism by hyperthermia. *Cancer Res.* 48, 4233–4239.
8. Ono, T., Kasamatsu, A., Oka, S., and Moss, J. (2006) The 39-kDa poly(ADP-ribose) glycohydrolase ARH3 hydrolyzes O-acetyl-ADP-ribose, a product of the Sir2 family of acetyl-histone deacetylases. *Proc. Natl. Acad. Sci. U.S.A.* 103, 16687–16691.
9. Juarez-Salinas, H., Sims, J. L., and Jacobson, M. K. (1979) Poly(ADP-ribose) levels in carcinogen-treated cells. *Nature* 282, 740–741.
10. Dantzer, F., Schreiber, V., Niedergang, C., Trucco, C., Flatter, E., De La Rubia, G., Oliver, J., Rolli, V., Menissier-de Murcia, J., and de Murcia, G. (1999) Involvement of poly(ADP-ribose) polymerase in base excision repair. *Biochimie* 81, 69–75.
11. Trucco, C., Oliver, F. J., de Murcia, G., and Menissier-de Murcia, J. (1998) DNA repair defect in poly(ADP-ribose) polymerase-deficient cell lines. *Nucleic Acids Res.* 26, 2644–2649.

12. Yu, S. W., Wang, H., Poitras, M. F., Coombs, C., Bowers, W. J., Federoff, H. J., Poirier, G. G., Dawson, T. M., and Dawson, V. L. (2002) Mediation of poly(ADP-ribose) polymerase-1-dependent cell death by apoptosis-inducing factor. *Science* 297, 259–263.
13. Jacobson, M. K., and Jacobson, E. L. (1999) Discovering new ADP-ribose polymer cycles: protecting the genome and more. *Trends Biochem. Sci.* 24, 415–417.
14. Haince, J. F., Rouleau, M., Hendzel, M. J., Masson, J. Y., and Poirier, G. G. (2005) Targeting poly(ADP-ribosylation): a promising approach in cancer therapy. *Trends Mol. Med.* 11, 456–463.
15. Evers, B., Drost, R., Schut, E., de Bruin, M., van der Burg, E., Derksen, P. W., Holstege, H., Liu, X., van Drunen, E., Beverloo, H. B., Smith, G. C., Martin, N. M., Lau, A., O'Connor, M. J., and Jonkers, J. (2008) Selective inhibition of BRCA2-deficient mammary tumor cell growth by AZD2281 and cisplatin. *Clin. Cancer Res.* 14, 3916–3925.
16. Fujihara, H., Ogino, H., Maeda, D., Shirai, H., Nozaki, T., Kamada, N., Jishage, K., Tanuma, S., Takato, T., Ochiya, T., Sugimura, T., and Masutani, M. (2009) Poly(ADP-ribose) Glycohydrolase deficiency sensitizes mouse ES cells to DNA damaging agents. *Curr. Cancer Drug Targets* 9, 953–962.
17. Gao, H., Coyle, D. L., Meyer-Ficca, M. L., Meyer, R. G., Jacobson, E. L., Wang, Z. Q., and Jacobson, M. K. (2007) Altered poly(ADP-ribose) metabolism impairs cellular responses to genotoxic stress in a hypomorphic mutant of poly(ADP-ribose) glycohydrolase. *Exp. Cell Res.* 313, 984–996.
18. Ame, J. C., Fouquerel, E., Gauthier, L. R., Biard, D., Boussin, F. D., Dantzer, F., de Murcia, G., and Schreiber, V. (2009) Radiation-induced mitotic catastrophe in PARG-deficient cells. *J. Cell Sci.* 122, 1990–2002.
19. Koh, D. W., Lawler, A. M., Poitras, M. F., Sasaki, M., Wattler, S., Nehls, M. C., Stoger, T., Poirier, G. G., Dawson, V. L., and Dawson, T. M. (2004) Failure to degrade poly(ADP-ribose) causes increased sensitivity to cytotoxicity and early embryonic lethality. *Proc. Natl. Acad. Sci. U.S.A.* 101, 17699–17704.
20. de Murcia, G., Huletsky, A., Lamarre, D., Gaudreau, A., Pouyet, J., Daune, M., and Poirier, G. G. (1986) Modulation of chromatin superstructure induced by poly(ADP-ribose) synthesis and degradation. *J. Biol. Chem.* 261, 7011–7017.
21. D'Amours, D., Desnoyers, S., D'Silva, I., and Poirier, G. G. (1999) Poly(ADP-ribosylation) reactions in the regulation of nuclear functions. *Biochem. J.* 342 (Part 2), 249–268.
22. Cook, B. D., Dynek, J. N., Chang, W., Shostak, G., and Smith, S. (2002) Role for the related poly(ADP-Ribose) polymerases tankyrase 1 and 2 at human telomeres. *Mol. Cell. Biol.* 22, 332–342.
23. Marchion, D. C., Bicaku, E., Daud, A. I., Sullivan, D. M., and Munster, P. N. (2005) Valproic acid alters chromatin structure by regulation of chromatin modulation proteins. *Cancer Res.* 65, 3815–3822.
24. Olive, P. L., Banath, J. P., and Durand, R. E. (1990) Heterogeneity in radiation-induced DNA damage and repair in tumor and normal cells measured using the “comet” assay. *Radiat. Res.* 122, 86–94.
25. Hartmann, A., Agurell, E., Beevers, C., Brendler-Schwaab, S., Burlinson, B., Clay, P., Collins, A., Smith, A., Speit, G., Thybaud, V., and Tice, R. R. (2003) Recommendations for conducting the in vivo alkaline Comet assay. 4th International Comet Assay Workshop. *Mutagenesis* 18, 45–51.
26. Satoh, M. S., and Lindahl, T. (1992) Role of poly(ADP-ribose) formation in DNA repair. *Nature* 356, 356–358.
27. Ravanat, J. L., Douki, T., and Cadet, J. (2001) Direct and indirect effects of UV radiation on DNA and its components. *J. Photochem. Photobiol. B* 63, 88–102.
28. Nunbhakdi, V., and Jacobson, E. L. (1987) Effects of a poly(ADP-ribose) polymerase inhibitor on mutation frequencies in dividing and quiescent C3H10T1/2 cells. *Mutat. Res.* 180, 249–256.
29. Pinsky, S. D., Tew, K. D., Smulson, M. E., and Woolley, P. V., III (1979) Modification of L1210 cell nuclear proteins by 1-methyl-1-nitrosourea and 1-methyl-3-nitro-1-nitrosoguanidine. *Cancer Res.* 39, 923–928.
30. Singh, N. P., McCoy, M. T., Tice, R. R., and Schneider, E. L. (1988) A simple technique for quantitation of low levels of DNA damage in individual cells. *Exp. Cell Res.* 175, 184–191.
31. Chhipa, R. R., Singh, S., Surve, S. V., Vijayakumar, M. V., and Bhat, M. K. (2005) Doxycycline potentiates antitumor effect of cyclophosphamide in mice. *Toxicol. Appl. Pharmacol.* 202, 268–277.
32. Ciocca, D. R., Fuqua, S. A., Lock-Lim, S., Toft, D. O., Welch, W. J., and McGuire, W. L. (1992) Response of human breast cancer cells to heat shock and chemotherapeutic drugs. *Cancer Res.* 52, 3648–3654.
33. Azab, S. S., El-Demerdash, E., Abdel-Naim, A. B., Youssef, E., El-Sharkawy, N., and Osman, A. M. (2005) Modulation of epirubicin cytotoxicity by tamoxifen in human breast cancer cell lines. *Biochem. Pharmacol.* 70, 725–732.
34. Mathis, G., and Althaus, F. R. (1986) Periodic changes of chromatin organization associated with rearrangement of repair patches accompany DNA excision repair of mammalian cells. *J. Biol. Chem.* 261, 5758–5765.
35. Adamietz, P. (1987) Poly(ADP-ribose) synthase is the major endogenous nonhistone acceptor for poly(ADP-ribose) in alkylated rat hepatoma cells. *Eur. J. Biochem.* 169, 365–372.
36. Panzeter, P. L., Realini, C. A., and Althaus, F. R. (1992) Noncovalent interactions of poly(adenosine diphosphate ribose) with histones. *Biochemistry* 31, 1379–1385.
37. Wesierska-Gadek, J., and Sauermann, G. (1988) The effect of poly(ADP-ribose) on interactions of DNA with histones H1, H3 and H4. *Eur. J. Biochem.* 173, 675–679.
38. Realini, C. A., and Althaus, F. R. (1992) Histone shuttling by poly(ADP-ribosylation). *J. Biol. Chem.* 267, 18858–18865.
39. David, K. K., Sasaki, M., Yu, S. W., Dawson, T. M., and Dawson, V. L. (2006) EndoG is dispensable in embryogenesis and apoptosis. *Cell Death Differ.* 13, 1147–1155.
40. Cortes, U., Tong, W. M., Coyle, D. L., Meyer-Ficca, M. L., Meyer, R. G., Petrilli, V., Herceg, Z., Jacobson, E. L., Jacobson, M. K., and Wang, Z. Q. (2004) Depletion of the 110-kilodalton isoform of poly(ADP-ribose) glycohydrolase increases sensitivity to genotoxic and endotoxic stress in mice. *Mol. Cell. Biol.* 24, 7163–7178.